Talanta 122 (2014) 135–139

Contents lists available at ScienceDirect

Talanta

journal homepage: www.elsevier.com/locate/talanta

A competitive electrochemical immunosensor for the detection of human interleukin-6 based on the electrically heated carbon electrode and silver nanoparticles functionalized labels

Yongbing Lou [a,1], Tingting He [b,c], Fang Jiang [b], Jian-Jun Shi [b,c], Jun-Jie Zhu [b,2]

[a] School of Chemistry and Chemical Engineering, Southeast University, Nanjing 211189, P. R. China
[b] State Key Lab of Analytical Chemistry for Life Science, School of Chemistry and Chemical Engineering, Nanjing University, Nanjing, 210093, P. R. China
[c] School of Chemical Engineering, Anhui University of Science and Technology, Huainan, 232001, China

ARTICLE INFO

Article history:
Received 18 October 2013
Received in revised form
8 January 2014
Accepted 11 January 2014
Available online 1 February 2014

Keywords:
HCPE
ERGO – AuPdNPs
IL-6
AgNPs
Immunosensor

ABSTRACT

A facile one-step electrochemical reduction method was developed to prepare electrochemically reduced graphene oxide (ERGO) and gold – palladium bimetallic nanoparticles (AuPdNPs) as the platform of immunosensor. A novel competitive electrochemical immunosensor was then proposed by combining the ERGO – AuPdNPs platform with silver nanoparticles (AgNPs) functionalized polystyrene bionanolabel for the sensitive detection of human interleukin-6 (IL-6). An electrically heated carbon electrode (HCPE) was introduced in the detection procedure of the immunosensor, and further improved the sensitivity. The immunosensor exhibited a wide linear response to IL-6 ranging from 0.1 to 100000 pg mL^{-1} with a detection limit of 0.059 pg mL^{-1}. The proposed method showed good precision, broad linear range, acceptable stability and high reproducibility, and could be used for the detection of IL-6 in real samples, which possessed promising application in clinical research.

1. Introduction

Human interleukin-6 (IL-6), an important cancer biomarker cytokine, associates with the development of multiple myeloma and leukemia [1–3]. According to research, IL-6 will be potential prognosticators to diagnose leukemia [4–6]. Therefore, the accurate and sensitive detection of IL-6 has become an intriguing subject in the study of mechanism, pathogenesis and earlier diagnosis of diseases. Traditionally, the expression of IL-6 in diseased tissues has been detected by enzyme-linked immunosorbent assay (ELISA) [7], fluorescent microarray [8], conductometric immunosensor [9], chemiluminescence immunoassay [10] and fluorescence-based fiber-optic biosensors [11]. Sophisticated instrumentation and relatively low limits of detection (LODs) for these methods restrict their further application for detecting early stage disease in real samples. Recently, various electrochemical techniques have been applied to construct IL-6 immunosensors with high sensitivity, good selectivity and low LOD [12–27]. For example, single wall carbon nanotubes forests with attached capture antibodies for IL-6 was constructed as an electrochemical sandwich immunoassay using enzyme label horseradish peroxidase to measure IL-6 by amperometric response in calf serum with a LOD of 0.5 pg mL^{-1} [14]. Deng prepared sensitive electrochemical immunosensor for the detection of IL-6 using enlarged and positively charged gold nanoparticles (AuNPs) to mediate electron transfer with LOD of 2 pg mL^{-1} [16]. A novel electrochemiluminescence immunosensor array featuring capture-antibody-decorated single-wall carbon nanotubes forests could detect IL-6 at a LOD of 0.25 pg mL^{-1} in serum [27]. An ultrasensitive electrochemical immunosensor based on silver nanoparticle (AgNP) – hollow titanium phosphate sphere labels combining with a magnetic sensing array had an extremely sensitive response to IL-6 in a linear range of 0.5–10000 pg mL^{-1} with a LOD of 0.1 pg mL^{-1} [17]. Immunosensor using electrically heated carbon electrode (HCPE) technique with AuNPs functionalized electroacitve labels had a detection range of 0.1–100 pg mL^{-1} with a LOD of 0.033 pg mL^{-1} [19]. Wang et al. fabricated a highly sensitive IL-6 amperometric immunosensor based on supersandwich multienzyme – DNA label, in which a LOD of 0.05 pg mL^{-1} was obtained [22].

Nevertheless, the sensitivity, response range, stability and selectivity still need to improve for IL-6 detection in clinical samples. Herein, a competitive dual signal amplification strategy was designed for electrochemical detection of IL-6, which integrated HCPE technique with AgNPs functionalized electroacitve labels. The HCPE technique is a wonderful way to accelerate reaction kinetic without changing the bulk solution temperature while it improves the mass transport by changing temperature of electrode, thus leading to an enhanced electrochemical signal

E-mail addresses: lou@seu.edu.cn (Y. Lou), jjzhu@nju.edu.cn (J.-J. Zhu).
[1] Tel.: +86 25 52090619; fax: +86 25 52090620.
[2] Tel.: +86 25 83597204; fax: +86 25 83594196.

0039-9140/$ - see front matter © 2014 Elsevier B.V. All rights reserved.
http://dx.doi.org/10.1016/j.talanta.2014.01.016

together with a higher signal-to-background ratio [28–31]. On the other hand, AgNPs for signal amplification in immunoassay show sharp and well-resolved sweeping voltammetry signals due to their unique recognition, transport and catalytic properties [32]. Particularly, compared with those quantum dots which are well recognized as electroacitve labels, the detection of AgNPs is easier and free of acid dissolution of metal ions. In addition, the fabrication of immunosensor needs the immobilization of a "receptor site", which selectively recognizes the analyte [33]. A simple, green and controllable electrochemical approach has been applied to fabricate the nanocomposite of electrochemically reduced graphene oxide and gold – palladium bimetallic nanoparticles (ERGO – AuPdNPs). This composite possesses the properties of the individual components with synergistic effect, which incorporates both the high-binding capability, excellent electrical and mechanical properties of graphene nanosheets, and favorable biocompatibility of AuNPs and PdNPs. Thereby ERGO – AuPdNPs are considered as the perfect platform material for immunosensors. The proposed immunosensor was successfully constructed with AgNPs as functionalized bionanolabel to detect IL-6, which exhibited attractive advantages such as broad response range, high sensitivity and specificity for the ultrasensitive detection of IL-6. It also gave satisfied results for real samples, revealing great potential towards early evaluation of cancer therapeutic effects.

2. Experimental

2.1. Chemicals and materials

IL-6 antigen, IL-6 antibody and IL-6 ELISA kit were purchased from Beijing Biosynthesis Biotechnology CO., LTD. 1-ethyl-3-(3-dimethylaminopropyl) carbodiimide hydrochloride (EDC), N-hydroxysuccinimide (NHS), dopamine and lyophilized bovine serum albumin (BSA) (99%) were purchased from Sigma – Aldrich. Polystyrene (PS) spheres of 200 nm in diameter were purchased from Northwestern Polytechnical University. Poly(acrylic acid) (PAA) was purchased from Jiangsu Huakang Chemicals Company (Nanjing, China). Silver nitrate ($AgNO_3$), chloroauric acid ($HAuCl_4$) and hexachloropalladic(IV) acid (H_2PdCl_6) were purchased from Shanghai Chemical Reagent Co. (Shanghai, China). Graphene oxide (GO) was prepared from graphite powder by a modified Hummers method as reported previously [34]. Phosphate buffer saline (PBS, 10 mM, pH 7.4) contained 136.7 mM NaCl, 2.7 mM KCl, 8.7 mM Na_2HPO_4 and 1.4 mM KH_2PO_4. The standard IL-6 antigen solution was prepared in the PBS and stored at 4 °C. All other chemicals were of analytical grade and used as received. All aqueous solutions were prepared using ultrapure water (Milli-Q, Millipore).

2.2. Apparatus

A CHI 760 electrochemical workstation and HCPE were used. The construction of HCPE has been reported elsewhere [19]. A function generator was used for heating, and the frequency was adjusted to 100 kHz in all heating experiments. Temperature of the HCPE was controlled by changing the output of the function generator. Morphology of the modified HCPE was verified by field-emission SEM (FESEM, HITACHI S4800). Transmission electron micrographs (TEM) were measured on a JEOL JEM 200CX transmission electron microscope, using an accelerating voltage of 200 kV. Electrochemical impedance spectroscopy (EIS) was performed with an Autolab electrochemical analyzer (Eco Chemie, The Netherlands) in a 10 mM $K_3Fe(CN)_6/K_4Fe(CN)_6$ (1:1) mixture with 1.0 M KCl as the supporting electrolyte, using an alternating current voltage of 5.0 mV, within the frequency range of 0.1 Hz–10 kHz. The static water contact angles were measured at 25 °C by a contact angle meter (Rame-Hart-100) employing drops of pure deionized water. The readings were stabilized and taken within 120 s after the sample addition.

2.3. Synthesis of the IL-6 – PS@PDA – AgNPs (PDA = polydopamine) bionanolabel

The preparation procedure for AgNPs functionalized labels (IL-6 – PS@PDA – AgNPs) is shown in Fig. 1A. 5 mg of PS spheres was sonicated in 3 mL Tris-HCl (pH 8.5) for several minutes and then centrifuged at 16000 rpm for 10 min. This washing procedure was repeated for three times. Then the PS spheres were dispersed in 10 mL Tris-HCl (pH 8.5) and sonicated for at least 30 min to form PS – Tris-HCl. PS@PDA was prepared according to literature method [35] by adding 20 mg dopamine into PS – Tris-HCl and then stirred for 24 h. This dispersion was centrifuged and washed twice with Tris-HCl (pH 8.5) and doubly distilled water. 2 mL of PS@PDA solution mixed with 4 mL of 0.5% PAA was sonicated for 2 h, and then centrifuged to discard the upper layer. The solid phase was washed with doubly distilled water twice. 10 mL of 0.02 M $AgNO_3$ was added and the mixture was sonicated for 24 h to form PS@PDA – AgNPs, and then centrifuged at 8500 rpm to remove the liquid portion. The PS@PDA – AgNPs was then dispersed into 2 mL of water and mixed with 0.5 mL PBS (pH 7.4) containing 400 mM EDC and 100 mM NHS to react at room temperature for 2 h. The mixture was then centrifuged at 15000 rpm and washed several times to remove excessive EDC and NHS. A total of 10 μL of 1 mg mL^{-1} IL-6 antigen (Ag) was added into the mixture and stirred for 6 h, then centrifuged at 12000 rpm at 4 °C for 10 min. A total of 500 μL PBS (pH 7.4) with 3% BSA was added into the bioconjugate to form a homogeneous dispersion (IL-6 – PS@PDA – AgNPs bionanolabel) and stored in the refrigerator at 4 °C before use.

2.4. Synthesis of ERGO – AuPdNPs

We develop a simple, green and controllable approach for electrochemical synthesis of ERGO – AuPdNPs nanocomposite as the immunosensor platform (Fig. 1B). 206 μL of 1% $HAuCl_4$ and 221.6 μL of 0.4% H_2PdCl_6 were dispersed into 50 mL of 0.9 mg mL^{-1} GO in $Na_2CO_3/NaHCO_3$ buffer solution (pH = 9.2) to form the electrodeposition electrolyte. The electrochemical reduction of GO, $HAuCl_4$ and H_2PdCl_6 was conducted in 200 μL electrolyte by repetitive cyclic voltammetry (CV) scanning from −1.5 V to 0.6 with a scan rate of 25 mV s^{-1} for 20 circles. The obtained ERGO – AuPdNPs nanocomposite was rinsed with PBS (50 mM, pH 7.4), dried at room temperature, and stored at 4 °C before use.

2.5. Fabrication of immunosensors

For the detection of IL-6, a competitive-type immunoassay was constructed as shown in Fig. 1B. ERGO – AuPdNPs modified HCPE was incubated in 20 μL of 100 mg L^{-1} anti-IL-6 for 12 h. After washing with PBS buffer, the Ab_1/ERGO – AuPdNPs/HCPE was incubated in 3% BSA and PBS solution at 37 °C for 1 h to block excess active groups and nonspecific binding sites on the surface. Then the electrode was incubated in solution containing a certain concentration of bionanolabel and 10 μl IL-6 Ag for 40 min. The IL-6 in the incubation solution competed with the IL-6 on the bionanolabel for the limited binding sites of immobilized anti-IL-6 on the surface of HCPE to form the immunocomplex. Finally, the electrode was washed thoroughly with PBS to remove nonspecifically bound Ab2 conjugates. The fabricated immunosensor was stored at 4 °C when not in use.

For electrochemical measurement, the immunosensor was incubated in 200 μL of 1.0 M KCl, and the silver component acting

as the detector target was quantified by linear sweep voltammetry (LSV). It is noteworthy that the concept of heated-electrode technique was introduced in the final stripping analysis for signal amplification.

3. Results and discussion

3.1. Characterization of platform and bionanolabel

Raman spectra (Fig. 2A) provide the evidence of successful preparation of ERGO. The Raman spectrum of graphene is usually characterized by two main features, the *G* mode arising from the first order scattering of the E_{2g} phonon of sp^2 C atoms (usually observed at $\sim$1575 cm^{-1}) and the *D* mode arising from a breathing mode of κ-point photons of A_{1g} symmetry ($\sim$1350 cm^{-1}) [36,37]. In our study, the *D* and *G* mode of graphene shifted to 1300 cm^{-1} and 1600 cm^{-1}, respectively. Additionally, the intensity ratio (I_D/I_G) of graphene in ERGO – AuPdNPs increased compared with pure GO, suggesting an increase of small in-plane sp^2 domains upon reduction of the exfoliated GO. SEM images can give further information on the morphology of the immunosensor surface during the modification process (Fig. 2B). It can be seen that the ERGO – AuPdNPs film was successfully built on the surface of HCPE and AuPdNPs were distributed homogeneously. Fig. 2C shows the TEM of the IL-6 – PS@PDA – AgNPs bioconjugates, illustrating the uniformity of the coating and the presence of the AgNPs on PS surface.

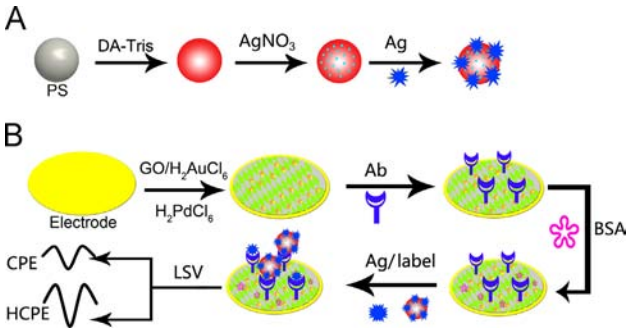

Fig. 1. (A) Assembly procedure of IL-6 – PS@PDA – AgNPs bionanolabel. (B) Schematic representation of the fabrication and measurement process of the competitive-type immunosensor.

The hydrophilicity of the electrode surface is commonly used to characterize its biocompatibility, which can be measured with the contact angle of the substrate. As shown in Fig. 3, the contact angles of the bare HCPE, ERGO/HCPE and ERGO – AuPdNPs/HCPE were $102.8 \pm 0.7^\circ$, $53.8 \pm 0.2^\circ$ and $15.4 \pm 0.1^\circ$, respectively. The ERGO – AuPdNPs film showed the lowest contact angle, indicating the best hydrophilicity. Thus, the improved biocompatibility of ERGO – AuPdNPs film was in favor of enhancing protein loading and retaining the bioactivity, which would improve the sensitivity of the immunosensor.

3.2. Electrochemical characteristics of the stepwise modified electrodes

The immunosensor fabrication process was characterized by the change of electrode-transfer resistance using $[Fe(CN)_6]^{3-/4-}$ as redox probes with EIS. Compared with bare HCPE (Fig. 4a), the charge transfer resistance (R_{ct}, the diameter of the semicircle in EIS) of ERGO – AuPdNPs/HCPE (Fig. 4b) decreased obviously, indicating that the ERGO – AuPdNPs film facilitated the diffusion of the $K_3[Fe(CN)_6]/K_4[Fe(CN)_6]$ redox probe towards the electrode surface. When anti-IL-6 (Fig. 4c) and BSA/anti-IL-6 (Fig. 4d) were absorbed onto the ERGO – AuPdNPs surface, the resistance increased consecutively, which was ascribed to the successive modifications of insulating proteins against the electron transfer on the electrode.

3.3. Optimization of electrochemical detection parameters

The concentration of the IL-6 – PS@PDA – AgNPs and the reaction time of the antigen-antibody conjugate could affect the analytical performance of the proposed immunosensor. As shown in Fig. 5A, with the increase of IL-6 – PS@PDA – AgNPs concentration, the peak current showed an increasing response until the IL-6 – PS@PDA – AgNPs volume reached 10 μL, indicating that all available recognition sites of immobilized anti-IL-6 could match with the nanoprobe. Thus, 10 μL was chosen as the optimal concentration. Moreover, at the optimized concentration, peak current changed with incubation time in the range of 10 $\sim$ 60 min, and reached a maximum value at 40 min (Fig. 5B). There exists an optimum incubation time which is probably due to the complete attachment of target protein, while the current decrease after longer time may be due to the deactivation of the protein. For

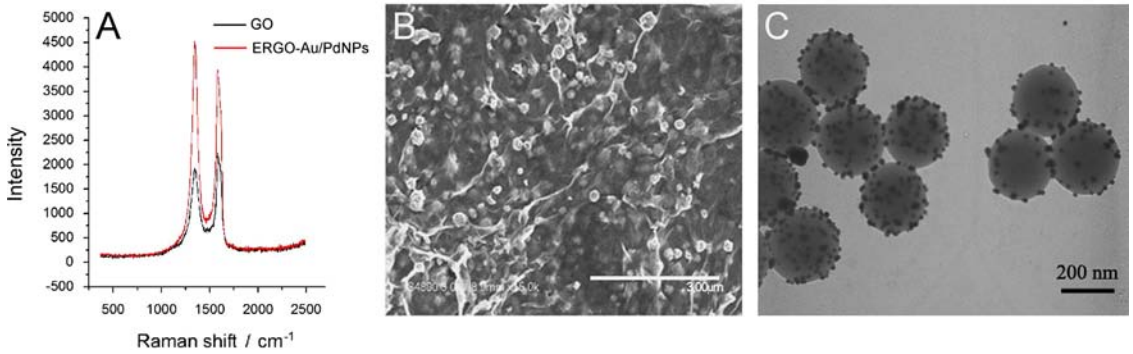

Fig. 2. (A) Raman spectra of GO and the prepared ERGO – AuPdNPs. (B) SEM image of the prepared ERGO – AuPdNPs. (C) TEM image of IL-6 – PS@PDA – AgNPs bionanolabel.

Fig. 3. Contact angle of (a) bare HCPE, (b) ERGO/HCPE, and (c) ERGO – AuPdNPs/HCPE.

sufficient recognition of target protein, 40 min was chosen as the optimal incubation time.

3.4. Performance of the immunosensor for IL-6

To evaluate the sensitivity and quantitative response range of the proposed immunoassay, we measured routine samples of different IL-6 concentrations using the developed competitive-type format immunoassay based on HCPE at a temperature of 49 °C. The LSV peak current of the immunosensor on HCPE decreased with the increasing IL-6 concentration in the incubation solution (Fig. 6A). The semi-log plot of peak current and IL-6 concentration showed a good linear relationship in the range from 0.1 to 100000 pg mL^{-1}, and the LOD was 0.059 pg mL^{-1} at a signal-to-noise of 3 (Fig. 6B, black line). For comparison, the amperometric response of the developed immunosensor was also recorded at room temperature (25 °C) by carbon paste electrode (CPE). However, the linear range of CPE system was only from 10 to 1000 pg mL^{-1} with a LOD of 2.45 pg mL^{-1} (Fig. 6B, red line). The high sensitivity and wide linear range of the proposed immunosensor were ascribed to the following reasons: (1) the dual signal amplification of AgNPs based bionanolabel and temperature-based signal enhancement by heated-electrode technique; (2) excellent biocompatibility, high electric conductivity and enhanced electron transfer kinetics of ERGO – AuPdNPs platform.

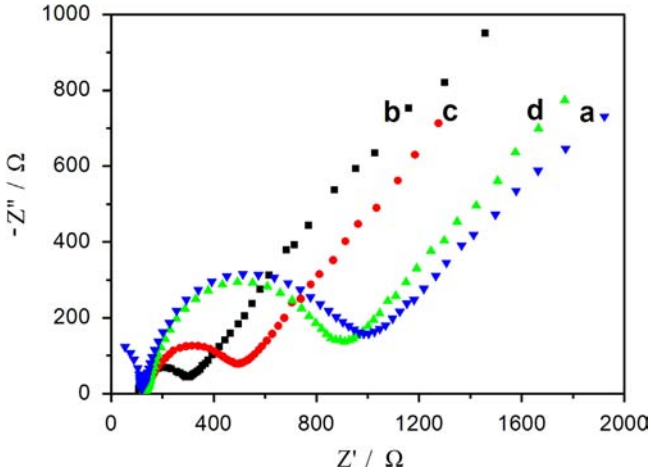

Fig. 4. EIS of (a) bare HCPE, (b) ERGO – AuPdNPs/HCPE, (c) anti-IL-6/ERGO – AuPdNPs/HCPE, and (d) BSA/anti-IL-6/ERGO – AuPdNPs/HCPE in 10.0 mM $[Fe(CN)_6]^{3-/4-}$ containing 1.0 M KCl.

3.5. Selectivity, reproducibility, stability and application

To investigate the specificity of the immunosensor, we mixed 10 pg mL^{-1} IL-6 with 100 pg mL^{-1} human BSA, 100 pg mL^{-1} cardiac troponin I (cTnI), 100 pg mL^{-1} carcinoembryonic antigen (CEA) and 100 pg mL^{-1} matrix metalloproteinase-2 (MMP-2), respectively. Compared to the immunosensor response in 10 pg mL^{-1} pure IL-6, no significant differences (R.S.D ranged from −6.5% to 10.9%) were observed for these samples, indicating that the human BSA, cTnI, CEA and MMP-2 could not cause observable interference (Fig. 7A). Furthermore, after the immunosensor was stored at 4 °C for 14 days, it remained more than 90% of initial responses for IL-6 (Fig. 7B). This result indicated the good stability of the immunosensor, which might be attributed to the

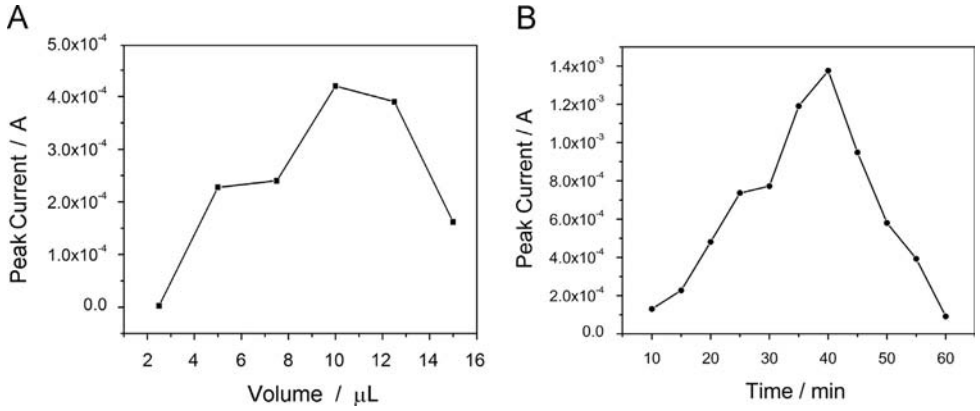

Fig. 5. Effects of IL-6 – PS@PDA – AgNPs concentration (A) and incubation time (B) on peak currents of LSV on HCPE for 100 pg mL^{-1} IL-6.

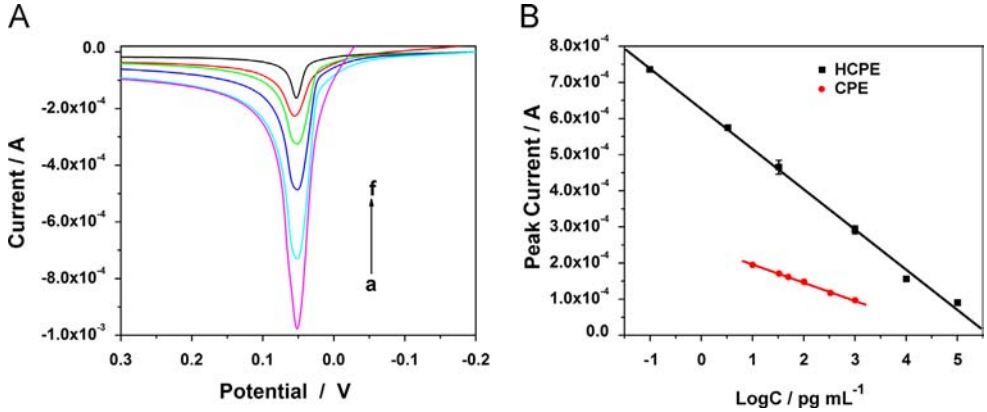

Fig. 6. (A) typical LSV responses of the immunosensor recorded on HCPE at temperature of 49 °C with IL-6 concentration from (a) to (f): 0, 0.1, 3.3, 33, 1000, 10000 pg mL^{-1}. (B) The resulting calibration curves of IL-6 plotted on a semi-log scale (the black line is heated at 49 °C and the red line is at room temperature about 25 °C).

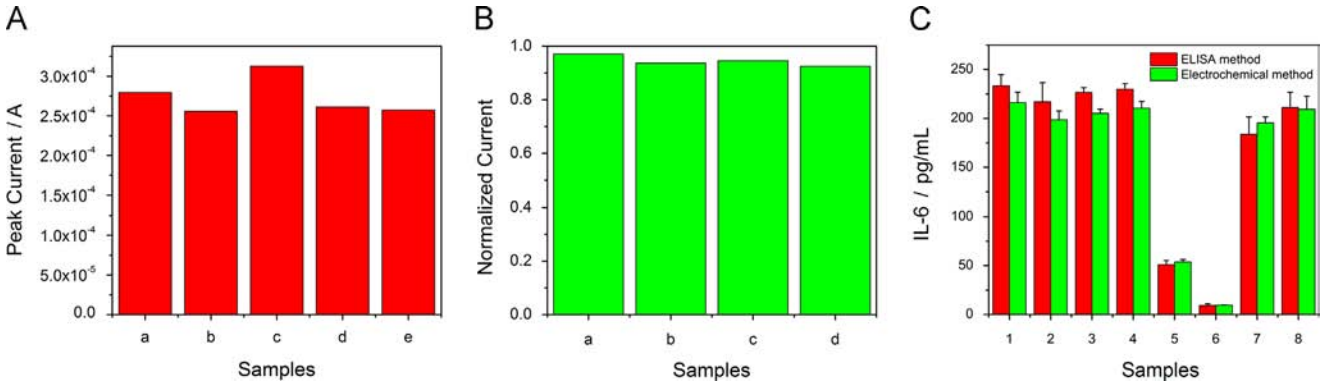

Fig. 7. (A) The specificity of the immunosensor for 10 pg mL^{-1} IL-6 towards other proteins: (a) pure IL-6, (b) with 100 pg mL^{-1}BSA, (c) with 100 pg mL^{-1} cTnI, (d) with 100 pg mL^{-1} CEA, and (e) with 100 pg mL^{-1} MMP-2. (B) Normalized currents of the immunosensor for 100 pg mL^{-1} IL-6 after 14 d storage: (a) control, (b)-(d) after 14 days. (C) Comparison of serum IL-6 levels determined using electrochemical immunoassay and ELISA method.

good biocompatibility of ERGO – AuPdNPs retaining the bioactivity of proteins. The slow decrease of responses might be due to the gradual deactivation of the immobilized biomolecules. The analytical reliability and application potential of the designed immunosensor was investigated by analyzing patient serum samples in comparison with the ELISA method. The results were listed in Fig. 7C, which showed a better performance than ELISA method and gave acceptable results with RSD less than 6.3%, indicating the feasibility of the proposed method for real samples.

4. Conclusion

In summary, a novel competitive electrochemical immunosensor, based on heated electrode technique combining high biocompatibility of ERGO – AuPdNPs as platform and the high sensitivity AgNPs as nanoprobe, was fabricated for the detection of human IL-6. The as-prepared immunosensor exhibited good reproducibility, acceptable stability, and a wide linear response range from 0.1 to 100000 pg mL^{-1} with a detection limit of 0.059 pg mL^{-1}. The immunosensor was also used to detect IL-6 in serum samples with satisfactory results. The attractive performance of this dual signal amplification strategy suggested potential application towards the early evaluation of tumor diseases.

Acknowledgements

This work was financially supported by the National Basic Research Program (2011CB933502) of China, and the National Natural Science Foundation of China (21335004, 21121091).

References

[1] P.C. Heinrich, I. Behrmann, S. Haan, H.M. Hermanns, G. Muller-Newen, F. Schaper, Biochem. J. 374 (2003) 1–20.
[2] L. Fayad, M.J. Keating, J.M. Reuben, S. O'Brien, B.N. Lee, S. Lerner, R. Kurzrock, Blood 97 (2001) 256–263.
[3] H. Isomoto, S. Kobayashi, N.W. Werneburg, S.F. Bronk, M.E. Guicciardi, D.A. Frank, G.J. Gores, Hepatology 42 (2005) 1329–1338.
[4] S. Perrier d'Hauterive, C. Charlet-Renard, M. Dubois, S. Berndt, F. Goffin, J.M. Foidart, V. Geenen, NeuroImmunoModulation 12 (2005) 157–163.
[5] D. Reynaud, E. Pietras, K. Barry-Holson, A. Mir, M. Binnewies, M. Jeanne, O. Sala-Torra, J.P. Radich, E. Passegue, Cancer Cell 20 (2011) 661–673.
[6] X. Wang, H.T. Wu, Z.X. Zhang, S.H. Liu, J. Yang, X.P. Chen, M. Fan, X.M. Wang, Cell. Mol. Neurobiol. 28 (2008) 113–124.
[7] C.K. Turner, T.M. Blieden, T.J. Smith, S.E. Feldon, D.C. Foster, P.J. Sime, R.P. Phipps, J. Immunol. Methods 291 (2004) 63–70.
[8] H. Wu, Q. Huo, S. Varnum, J. Wang, G. Liu, Z. Nie, J. Liu, Y. Lin, Analyst 133 (2008) 1550–1555.
[9] K. Liang, W. Mu, M. Huang, Z. Yu, Q. Lai, Electroanalysis 18 (2006) 1505–1510.
[10] L.R. Luo, Z.J. Zhang, L.Y. Hou, J. Wang, W. Tian, Talanta 72 (2007) 1293–1297.
[11] R. Kapoor, C.W. Wang, Biosens. Bioelectron. 24 (2009) 2696–2701.
[12] G.A. Messina, N.V. Panini, N.A. Martinez, J. Raba, Anal. Biochem. 380 (2008) 262–267.
[13] B.S. Munge, C.E. Krause, R. Malhotra, V. Patel, J.S. Gutkind, J.F. Rusling, Electrochem. Commun. 11 (2009) 1009–1012.
[14] R. Malhotra, V. Patel, J.P. Vaque, J.S. Gutkind, J.F. Rusling, Anal. Chem. 82 (2010) 3118–3123.
[15] B.V. Chikkaveeraiah, V. Mani, V. Patel, J.S. Gutkind, J.F. Rusling, Biosensors Bioelectron 26 (2011) 4477–4483.
[16] C. Deng, F. Qu, H. Sun, M. Yang, Sens. Actuators, B 160 (2011) 471–474.
[17] J. Peng, L.N. Feng, Z.J. Ren, L.P. Jiang, J.J. Zhu, Small 7 (2011) 2921–2928.
[18] G. Wang, H. Huang, G. Zhang, X. Zhang, B. Fang, L. Wang, Langmuir 27 (2011) 1224–1231.
[19] J.J. Zhang, Y. Liu, L.H. Hu, L.P. Jiang, J.J. Zhu, Chem. Commun. 47 (2011) 6551–6553.
[20] R. Malhotra, V. Patel, B.V. Chikkaveeraiah, B.S. Munge, S.C. Cheong, R.B. Zain, M.T. Abraham, D.K. Dey, J.S. Gutkind, J.F. Rusling, Anal. Chem. 84 (2012) 6249–6255.
[21] C.K. Tang, A. Vaze, J.F. Rusling, Lab Chip 12 (2012) 281–286.
[22] G. Wang, H. Huang, B. Wang, X. Zhang, L. Wang, Chem. Commun. 48 (2012) 720–722.
[23] T. Yang, S. Wang, H. Jin, W. Bao, S. Huang, J. Wang, Sens. Actuators, B 178 (2013) 310–315.
[24] K.-Z. Liang, W.-J. Mu, Chem. Lett. 37 (2008) 1078–1079.
[25] K.Z. Liang, J.S. Qi, W.J. Mu, Z.X. Liu, Bioprocess Biosyst. Eng. 32 (2009) 353–359.
[26] T. Li, M. Yang, Sens. Actuators, B 158 (2011) 361–365.
[27] N.P. Sardesai, J.C. Barron, J.F. Rusling, Anal. Chem. 83 (2011) 6698–6703.
[28] M. Jasinski, A. Kirbs, M. Schmehl, P. Gründler, Electrochem. Commun. 1 (1999) 26–28.
[29] G.-U. Flechsig, O. Korbout, S.B. Hocevar, S. Thongngamdee, B. Ogorevc, P. Gründler, J. Wang, Electroanalysis 14 (2002) 192–196.
[30] R. Cui, H. Huang, Z. Yin, D. Gao, J.J. Zhu, Biosens. Bioelectron. 23 (2008) 1666–1673.
[31] M. Jacobsen, H. Duwensee, F. Wachholz, M. Adamovski, G.-U. Flechsig, Electroanalysis 22 (2010) 1483–1488.
[32] S. Kittler, C. Greulich, J.S. Gebauer, J. Diendorf, L. Treuel, L. Ruiz, J.M. Gonzalez-Calbet, M. Vallet-Regi, R. Zellner, M. Koller, M. Epple, J. Mater. Chem. 20 (2010) 512–518.
[33] A. Kausaite-Minkstimiene, A. Ramanaviciene, J. Kirlyte, A. Ramanavicius, Anal. Chem. 82 (2010) 6401–6408.
[34] K. Liu, J. Zhang, G. Yang, C. Wang, J.-J. Zhu, Electrochem. Commun. 12 (2010) 402–405.
[35] B. Yu, D.A. Wang, Q. Ye, F. Zhou, W. Liu, Chem. Commun. 45 (2009) 6789–6791.
[36] A.C. Ferrari, J.C. Meyer, V. Scardaci, C. Casiraghi, M. Lazzeri, F. Mauri, S. Piscanec, D. Jiang, K.S. Novoselov, S. Roth, A.K. Geim, Phys. Rev. Lett. 97 (2006) 187401.
[37] A.A. Balandin, S. Ghosh, W. Bao, I. Calizo, D. Teweldebrhan, F. Miao, C.N. Lau, Nano Lett. 8 (2008) 902–907.